MULTIDISCIPLINARY DESIGN OPTIMIZATION OF WING STRUCTURE FOR STRUT-BRACED WING AIRCRAFT CONSIDERING AEROELASTICITY

Wang Zexi[1], Wan Zhiqiang[1], Yang Chao [1] and Zhu Siyan [1]

[1] School of Aeronautic Science and Engineering, Beihang University
Key Laboratory of Aircraft Advanced Design Technology (Beihang University)，Ministry of Industry and Information Technology
wangzexi@buaa.edu.cn

Keywords: strut-braced wing, conceptual design, composite structure, aeroelasticity, multidisciplinary design optimization, genetic algorithm

Abstract:
The potential benefits of composite wing structure can be more largely developed through detailed analyses on the inherent features of fluid-structure coupling in conceptual stage. A multidisciplinary design optimization (MDO) method on composite wing structure of strut-braced wing (SBW) commercial aircraft is proposed. The object of optimization is to minimum structure weight and aeroelastic indices including wing tip displacement, aerodynamic twist, aileron effectiveness, laminate strain, composite failure as well as buckling are taken into consideration as design constrains. The effects of configuration parameters, composite laminate thickness and section size of main beams are taken into comprehensive consideration in this method based on genetic algorithm. Aerodynamic analysis of whole aircraft in cruise state is based on solving Eular equations and drag prediction can be obtained by a viscous correction method, which is confirmed suitable for genetic optimization. The results demonstrate that aeroelasticity as well as composite structure significantly effects aerodynamic performance and should be taken into consideration in conceptual stage.

1 INTRODUCTION

Aircraft with cantilever wing have been greatly improved in the flight performance and efficiency, compared to the early models. However, limited to its structural form that forces all the flight load to transfer to wing root through shear and bending moment, the weight of wing structure grows drastically as the wing span increases. Furthermore, the reduction of wave drag during transonic flight increases wing sweep, which reduces aerodynamic efficiency as well as increases structural weight. Thus, it is quite promising to study the new configuration of the transonic vehicle for further improvement on performance and efficiency.

The strut-braced wing aircraft or also called truss-braced wing (TBW) aircraft have attached truss in the middle of the wing structure, which overcomes such disadvantages of cantilever aircraft [1-4]. Larger span and less structure weight could be gained benefiting from its unique configuration, in which less flight load would be beard by main wing structure. [5] Simultaneously, a thinner airfoil could be achieved for the same reason, therefore reduces shock wave interference during transonic flight, which makes a reduction of wing sweep available, at the same time parasitic drag decreases due to an increase of natural laminar flow [6]. For these reasons, SBW aircraft require less thrust comparing to cantilever aircraft for the same flight profile, therefore less fuel consumption as well as less pollution emissions could be achieved. It is worth mentioning that SBW aircraft would produce less noise, which is significant for urban airports.

Committing to those advantages, SBW aircraft have been studied since 1950s by several research institutes like NASA and Boeing [7-8]. Despite all the great progress they have made during several decades, the elastic deformation of structure was insufficiently studied. Due to reduction of stiffness, wing structure performed a much greater displacement as well as torsion in the same flight condition, and inertial force as well as aerodynamic force affects more deeply on structure. Unfortunately, the character of strut makes this fluid-structure coupling system much more complicated, and then leads the displacement as well as torsion which would affect aerodynamic load distribution in turn, to be much more difficult to approach without taking the elasticity of structure into consideration. Thus, aeroelasticity in SBW aircraft is significant due to such tight coupling of structure and aerodynamics.

Furthermore, the early studies mostly focused on aerodynamic and the structure part was inevitably taken into less consideration: on the one hand, the wing weight was calculated by empirical estimation therefore there is potential in better accuracy; on the other hand, the composite structure with high specific strength as well as high specific stiffness was not applied to main bearing structure, which could offer a greater weight reduction. Hence a more accurate and practical optimization result could be obtained after applying composite materials to main bearing structure. However, applying of composite laminate greatly increases the complexity of design and makes it impossible to design every section of laminate manually. Besides, the laminate of cantilever wing provides very limited reference for SBW due to the huge configuration change. Based on these challenges, optimization became a suitable and necessary way to deal with the massive and close-contacted design variables. Moreover, the constraints required by several different disciplines highlights the incompetence of traditional optimize methodology, which optimizes parameters individually and lack of ability to consider variety of conditions at same time, hence making it not qualified for multi-condition requirement. Therefore, the multidisciplinary design optimization (MDO) methodology which is a convincing tool to get the most valuable design considering the synergism of all those parameters, would make this kind of design achievable. MDO could show a better view of design space and make designers more deeply informed of overall situations [2-5]. Apparently, the result approached by MDO would provide a better guidance for conceptual design especially in structural stiffness distribution and relative parameters. In addition, considering the serious drain on computing, proposing a time-saving methodology would be significant for practical engineering.

2 METHODOLOGY

2.1 Aeroelastic Response Analysis

The aeroelastic response analysis in this method includes static aeroelasticity analysis and flutter analysis.

2.1.1 Equation for Static Aeroelastic Analysis

The basic equation for static aeroelastic analysis is [9]

$$\boldsymbol{K}_{aa}\boldsymbol{u}_a + \boldsymbol{M}_{aa}\ddot{\boldsymbol{u}}_a - \bar{q}\boldsymbol{Q}_{aa}\boldsymbol{u}_a = \bar{q}\boldsymbol{Q}_{ax}\boldsymbol{u}_x + \boldsymbol{P}_a \tag{1}$$

where $\boldsymbol{K}_{aa}$ is the matrix of structure stiffness (where subscript *a* means analysis-freedom), $\boldsymbol{M}_{aa}$ is the matrix of structural mass, $\boldsymbol{Q}_{aa}$ is the matrix of aerodynamic influence coefficient(AIC), $\bar{q}$ is the dynamic pressure of incoming flow, $\boldsymbol{u}_a$ is the vector if structural deformation, $\boldsymbol{u}_x$ is the vector of additional freedom for aerodynamic trim parameters including angle of attack, sideward acceleration and pitch attitude ratio, which is used to define overall rigid motion of aircraft and deflection of aerodynamic control surfaces, and $\boldsymbol{P}_a$ is the vector of applied loads. In this equation, the item $\bar{q}\boldsymbol{Q}_{aa}\boldsymbol{u}_a$ refers to the increment aerodynamic force caused by elastic deformation of structure, which exerts significant influence in this very-high aspect ratio model.

2.1.2 Equation for Flutter Analysis

The equation of *p*-*k* flutter analysis method used in this method is [10]:

$$\left[\left(\frac{V}{b}\right)^2 p^2\boldsymbol{M} + \frac{V}{b}p\boldsymbol{B} + \boldsymbol{K} - \frac{1}{2}\rho V^2\left(\boldsymbol{Q}^R + \frac{p}{k}\boldsymbol{Q}^I\right)\right]\boldsymbol{u} = 0 \qquad (2)$$

Where ***M*** is the matrix of generalized structural degree of freedom, ***B*** is the matrix of generalized damping, ***K*** is the matrix of generalized structral stiffness, ***Q*** is the matrix of generalized unsteady aerodynamic force, *V* is the speed of incoming slow, *b* is the length of reference chord, *p* is teh eigenvalure, *k* is the density of air, *u* is the reduced frequence, ***u*** is the vector of generalized structral degree of freedom. The superscripts *R* and *I* represent the real part and the imaginary part, respectively.

2.2 Geometric Parameterization

Geometric parameterization is necessary to make configuration optimization achievable.

Table 1: Symbol and Description for Design Variables of Geometric Parameterization

Number	Symbol	Description
1	l	Semispan
2	χ	Wing weep
3	c_{root}	Wing root chord
4	c_{tip}	Wing tip cord
5	K_s	Span wise position of wing-strut intersection
6	K_e	Span wise position of engine
7	ψ	Dihedral angle

Design variables of configuration are shown in Table 1 and intuitively shown in Figure 1 as a supplement. The parameters that have significant effects on flight performance and structure weight have been taken into consideration including semispan, wing sweep, wing root chord, wing tip chord. Span wise position of wing-strut intersection is also closely related to load distribution therefore should be studied as well. The sectional shape of airfoil remains unchanged in the process of geometric parameter changing and deformation interpolation.

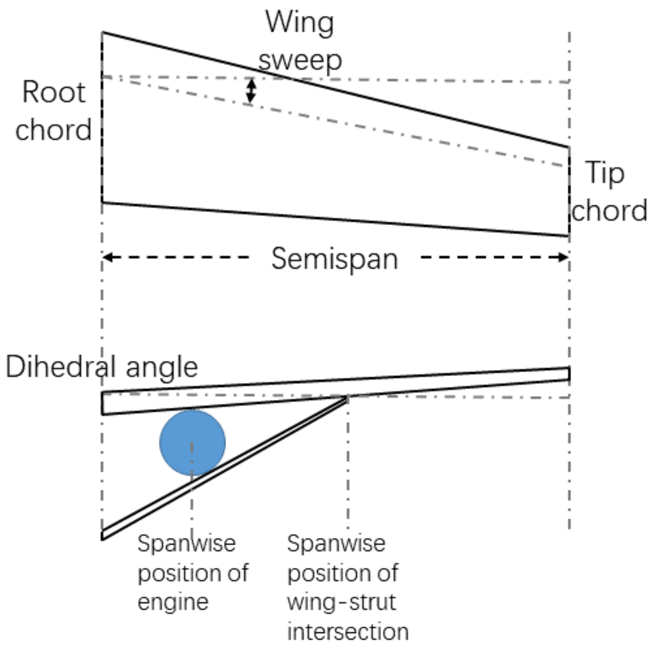

Figure 1: Design Variables for Configuration Optimization

2.3 Failure Analysis

The rationality of structural stiffness and strength in conceptual stage plays an important guiding role in the following-up study, which makes failure analysis an important constraint that must be taken into consideration. The failure criteria for composite structure used in this method is Tsai-Wu failure criteria, which presents a theoretic strength assessment method for anisotropic materials. The equation of this method can be descripted as:

$$F_{11}\sigma_1^2 + 2F_{12}\sigma_1\sigma_2 + F_{22}\sigma_2^2 + F_{66}\sigma_{12}^2 + F_1\sigma_1 + F_2\sigma_2 = 1 \quad (3)$$

Five of those parameters in Eq.(3) could be measured in tensile or compressive experiments along the principal material directions as follows:

$$F_1 = \frac{1}{X_t} - \frac{1}{X_c}, F_2 = \frac{1}{Y_t} - \frac{1}{Y_c}, F_{11} = \frac{1}{X_t X_c}, F_{22} = \frac{1}{Y_t Y_c}, F_{66} = \frac{1}{S^2},$$

where X_t and X_c are the allowable tensile and compressive stresses along the principal *x* direction of the material respectively, Y_t and Y_c are the allowable tensile and compressive stresses along the principal *y* direction of the material respectively, and *S* is the allowable shear stress in the principal material coordinate system.

The interaction term F_{12} in Eq.(3) must be evaluated experimentally and constrained by stability criterion $F_{11}F_{22} - F_{12}^2 > 0$. However, an experimental study [12] shows that there is no discernible difference across the full range of values of the interaction term from -1 to 1. Narayanaswami and Adelman [13] suggested that the use of Tsai-Wu failure criteria with $F_{12} = 0$ is a preferred alternative to experimentally determining F_{12}. When applied to assess the strength of composite structure, the failure indices of laminates are obtained by the left side of Eq.(3). If the absolute value of this index is larger than 1.0, the corresponding laminate ply is considered to be failure. Hence the design constrain of failure indices is generally set to be [-1.0, 1.0].

2.4 Aeroelastic Optimization

In this paper, the optimization study taken into consideration of aeroelasticity and aerodynamic can be descripted as following mathematic problem, which is [10]:
minimize

$$F(\boldsymbol{v}) = F(v_1, v_2, \cdots v_n) \tag{4}$$

subject to

$$(c_i)_{\text{lower}} \le g_j(\boldsymbol{v}) \le (c_i)_{\text{upper}} \qquad j = 1, \ldots, n_c \tag{5}$$

$$(v_i)_{\text{lower}} \le v_i \le (v_i)_{\text{upper}} \qquad i = 1, \ldots, n_d \tag{6}$$

where $F(v)$ is the objective function of design variables, which is the structural weight in this research. Eq. (5) is used to define optimization constrains, where $g_j(\boldsymbol{v})$ are the responses to aeroelastic analyses, $(c_i)_{\text{lower}}$ and $(c_i)_{\text{upper}}$ are the lower and upper bounds of design constrains respectively. Eq. (6) defines the feasible domain of design variables.

The penalty function is a common method for calculation of constraint fitness and can be expressed as [13]:

$$R_j(\boldsymbol{v}) = \begin{cases} \exp\left(\dfrac{\left|g_j(\boldsymbol{v}) - (c_j)_{lower}\right|}{\left|(c_j)_{lower}\right| + 1.0}\right) & g_j(\boldsymbol{v}) \le (c_j)_{lower} \\ 1.0 & (c_j)_{lower} \le g_j(\boldsymbol{v}) \le (c_j)_{upper} \\ \exp\left(\dfrac{\left|g_j(\boldsymbol{v}) - (c_j)_{upper}\right|}{\left|(c_j)_{upper}\right| + 1.0}\right) & (c_j)_{upper} \le g_j(\boldsymbol{v}) \end{cases} \tag{7}$$

where $R_j(\boldsymbol{v})$ is the fitness of the *j*th constraint. In this method, the fitness is 1.0 if $g_j(\boldsymbol{v})$ stratifies the given constraint, otherwise the fitness is lower than 1.0. The expression of this penalty function decides that the more each response value deviates from the constraint bound, the lower the corresponding fitness will be obtained.

2.5 CFD Solving Method

The MGAERO (Multi-Grid AEROdynamics) software is applied for CFD analysis in this method. The use of Cartesian grid cells, which may be sheared or rotated, effectively eliminates the labor-intensive task of grid generation [14]. The most significant advantage is that there is no relation required between the surface paneling and the local grid cell structure [16], which means all the grids can generated automatically through geometric parameters calculated by genetic algorithm. Therefore, the MGAERO code is suitable for a genetic algorithm based optimization.

The MGAERO code solves the Euler equations in three dimensions using standard central differencing techniques [15]. The integral form of Euler equations for general control volume *Vol* can be expressed as following:

$$\frac{\partial}{\partial t}\iiint_{Vol} \boldsymbol{F} dv + \iint_S \vec{\boldsymbol{E}} \cdot \boldsymbol{n} dS = 0 \tag{8}$$

where $\boldsymbol{F} = [\rho, \rho u, \rho v, \rho w, \rho e]^T$, ρ is the density of flow, *u*, *v* and *w* are the velocity components in Cartesian coordinate system, *e* is the internal energy of unit volume, ***n*** is the outward normal vector, and $\vec{\boldsymbol{E}}$ is the flux vector. Besides the induced drag, the shock drag can be calculated as well [16]. The application of a modified 4-stage Runge-Kutta time marching scheme accelerates convergence to a steady state.

A viscous correction method based on Euler equations is applied to analysis the viscous drag. The viscous correction is available via an integral boundary calculation along surface streamlines [17]. The application of inviscid-viscous iteration method improves the accuracy of aerodynamic analysis, and the low compute cost is satisfied for conceptual design.

3 OPTIMIZATION DESCRIPTION

3.1 Structural and aerodynamic models

The structural model of SBW aircraft in conceptual stage is shown in Figure 2. The structural stiffness is simulated by rod elements and quadrilateral elements, which are applied beam properties and composite properties, respectively. The offset value to symmetrical surface of composite laminates is simulated by a ply with very small stiffness. Therefore, the bending and torsional stiffness of real composite wing structure can be approximated with few deviations. The weight of fuel and other non-structural mass are simulated by lumped mass distributed along beam elements. The way that strut and wing structure intersected is simulated by an MPC element [18], which is setup to keep the displacement components of wing structure and strut consistent at the intersection position rather than twist components. Therefore, only support or pulling force is provided for wing structure by strut and the bending moment of wing structure is not passed to strut. The aerodynamic model corresponding to structure model of SBW aircraft is shown in Figure 3.

The jig shape, which is not deformed, is generated geometrically. Then the cruise shape used for aerodynamic analysis, which represents the deformed wings in cruise condition, is interpolated based on the displacement of structural grids calculated by aeroelastic analysis. The difference between jig shape and cruise is shown in Figure 4.

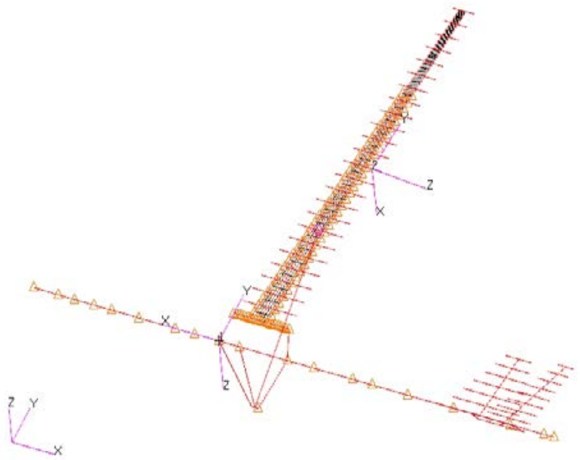

Figure 2: Structure model of SBW aircraft

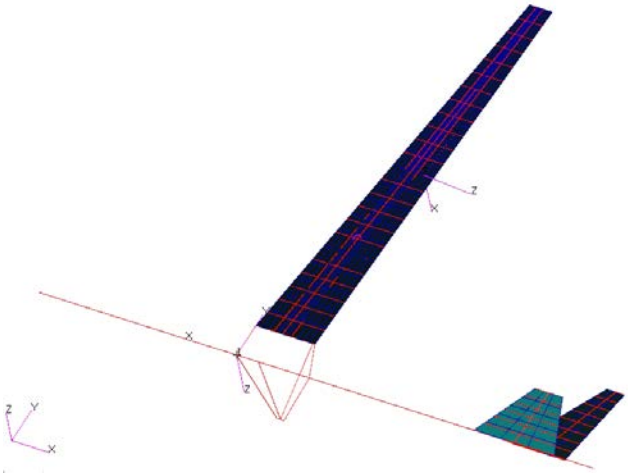

Figure 3: Aerodynamic model for aeroelastic analysis of SBW aircraft

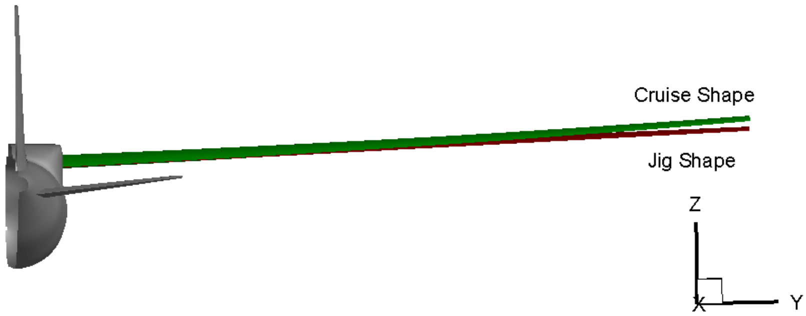

Figure 4: Jig shape and cruise shape of aerodynamic model

The analysis of normal modes is applied on structure therefore the rationality of structure is verified. The first eight normal modes of wing-strut structure are shown in Figure 5 and the frequency of each model is shown in Table 2. Due to the influence of strut, the vertical bending stiffness of wing-strut increases, therefore the frequency of first vertical bending mode increases and very close to the frequency of first horizontal bending mode.

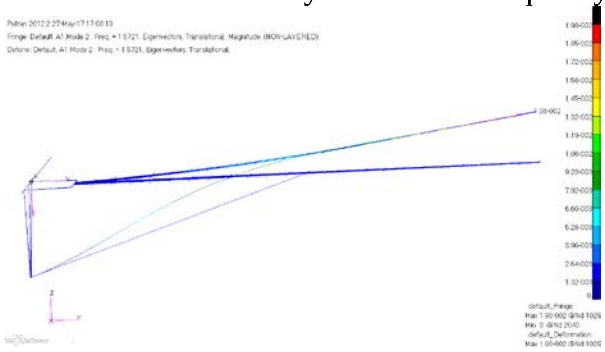

(a) First vertical bending model

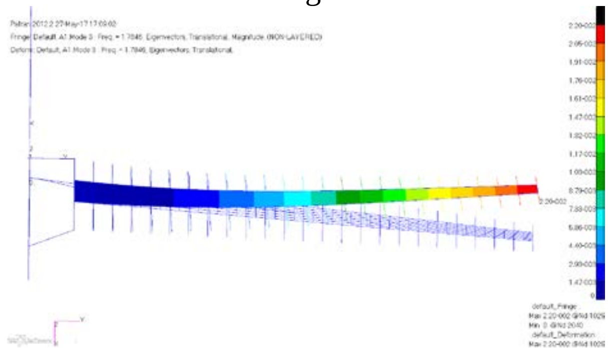

(b) First horizontal bending model

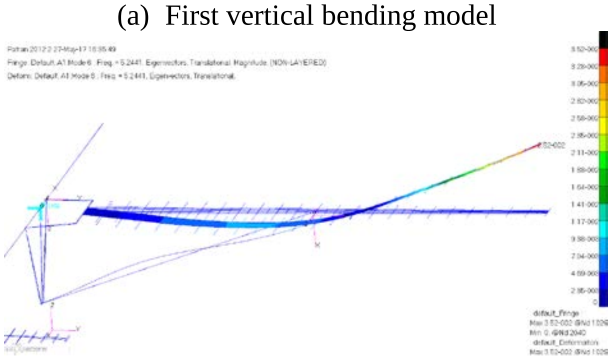

(c) Second vertical bending mode

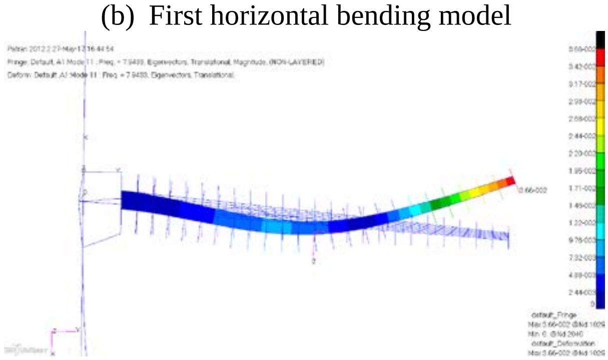

(d) Second horizontal bending mode

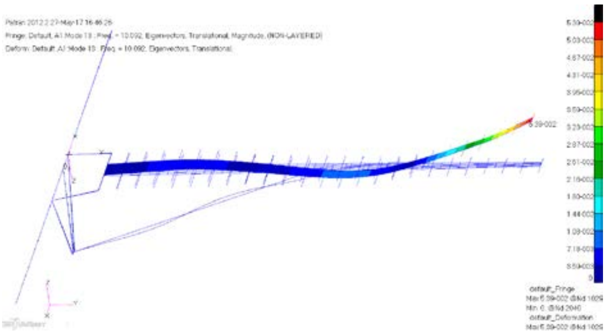

(e) Third vertical bending mode

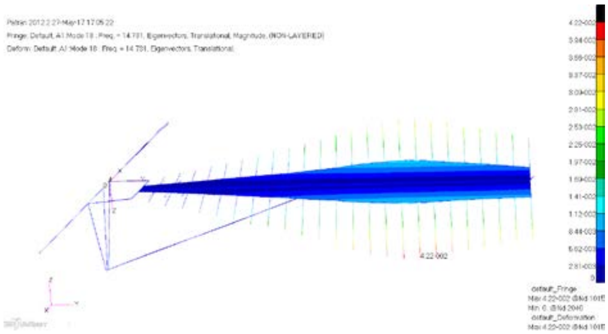

(f) First torsion mode

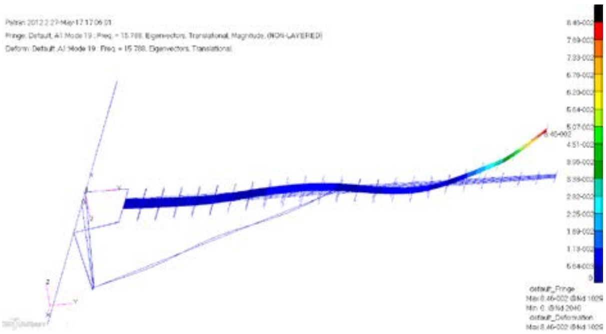

(g) Forth vertical bending mode

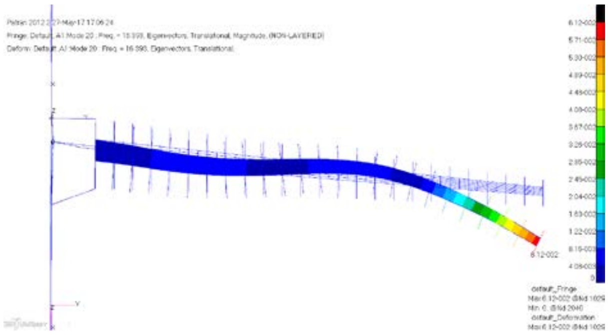

(h) Third horizontal bending mode

Figure 5: First eight normal modes of wing-strut structure

Table 2: Frequency of first eight normal modes

Mode	Description	Frequency, Hz
1	First vertical bending	1.5721
2	First horizontal bending	1.7846
3	Second vertical bending	5.2441
4	Second horizontal bending	7.9433
5	Third vertical bending	10.092
6	First torsion	14.731
7	Forth vertical bending	15.788
8	Third horizontal bending	16.393

3.2 Optimization Strategy

The cruise subcase is Ma=0.6 at the altitude of 8.0km, and the total weight of the full-model aircraft is 98,000 kg (216053 lb.). The position of strut-wing intersecting position effects the form of structure deformation, which makes it different from other configuration design variables, thus should be taken into consideration individually. In order to study the influence of strut-wing intersecting position, four typical position is chosen and a genetic algorithm is applied on the other design variables with the combination of each strut-wing intersecting position.

Structure design part focusing on central wing box contains thickness of skin on central box and sectional size of beam, which together effect the stiffness and deformation significantly. The symmetric balanced laminate is applied for composite skin and aeronautical aluminum alloy is applied for beams. The thickness ratio of 0°, 45°, -45°and 90° laminate is 5:2:2:1.

Upper skin is divided into 8 independent sections along span wise in total. Thickness of skin is set to continuously increase from tip to root considering the little mutation of bending moment on wing-strut intersection position compared to the whole flight load, as well as the technological requirements of composite laminate. Likewise, the lower skin is treated using the same strategy. The front and rear beams are divided into 8 sections only along span, and the sectional size changes in the same fashion as the skin. The middle beam is applied from root of the wing and ends to 75% length of simespan, for the load is relatively smaller in the outer part of the wing. Strut sectional area is also a structure design variable that affects the stiffness. All of 31 structure design variables are set up in design space.

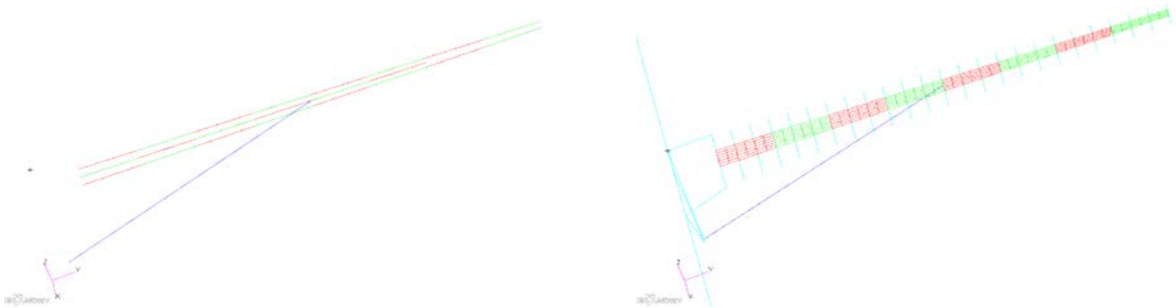

(a) Regional division of beam and strut (b) Regional division of composite

Figure 6: Regional division of wing-strut structure

Design constraints are set up to ensure the optimization results meet the multidisciplinary requirements of given flight mission. Static deformation and wingtip torsion angle mainly considered in the subcase of 2.5g load, while other aeroelastic indices such as aileron efficiency and flutter speed are checked. Composite strain constraint and failure constraint are the essential constraints of composite skin. Buckling of strut have been taken into consideration in negative load case. All constraints are shown in Table 3.

Table 3: Design constraints for optimization

Number	Description	Constraint
1	Static deformation constraint	Tip displacement<12% of semi span, 2.5g load
2	Wingtip torsion angle constraint	$\leq 4.5°$, 2.5g load
3	Aileron efficiency constraint	$\geq 65\%$
4	Flutter speed constraint	$\geq 300 m/s$
5	Composite strain constraint	$-3500\mu\varepsilon \leq \text{Strain} \leq 3500\mu\varepsilon$
6	Composite failure constraint	Tsai-Wu failure criterion, $-1 < \text{factor} < 1$ $-1 < \text{factor} < 1$
7	Strut strength constraint	$\sigma < 400 Mpa$
8	Strut buckling constraint	Margin of Safety > 0

3.3 Optimization Flowchart

The genetic optimization parameters including population size, number of generations, coding mode, convergence criterion and probabilities of crossover and mutation are defined before starting of optimization [19]. The initial generation is generated randomly, while the subsequent generations are generated based on the fitness assessment of previous ones and appropriate variation of design variables. Convergence judgment is applied through overall analysis of each generation, and the optimization will terminate if convergence criteria is met.

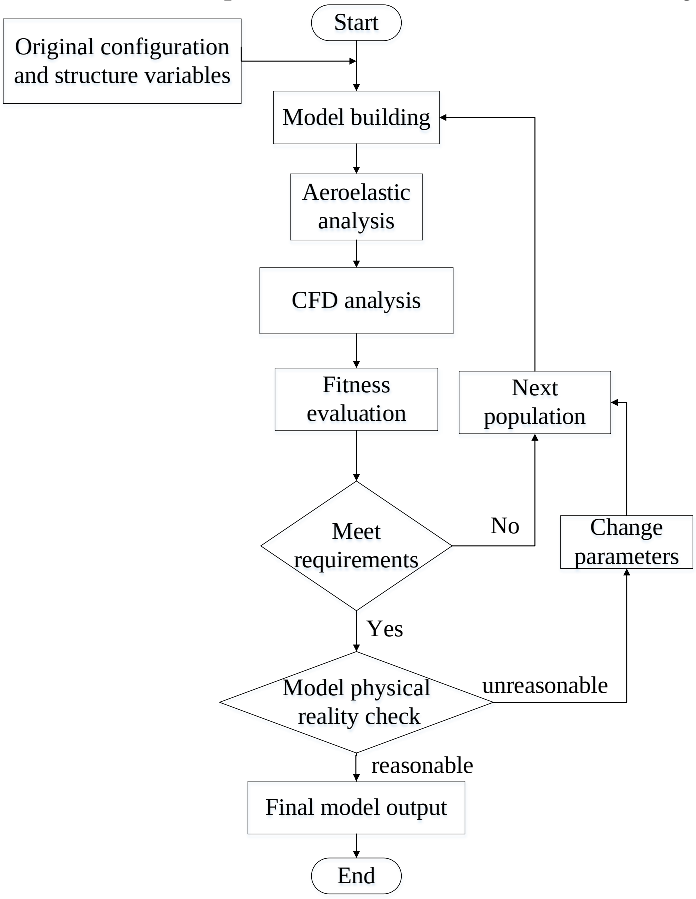

Figure 7: Optimization flowchart for MDO design considering aeroelasticity and aerodynamic performance

4 RESULT

4.1 Static aeroelastic analysis

The result of aerodynamic analysis in cruise condition is shown in Figure 8.

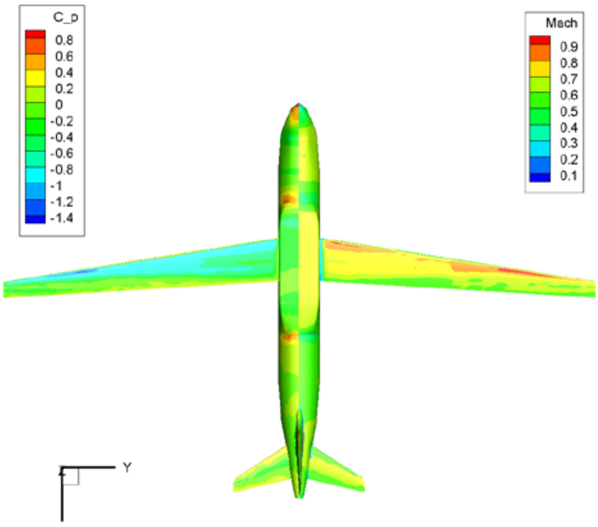

Figure 8: Surface C_p and Mach number distribution in cruise condition

The static aeroelastic analysis of a baseline model is applied to verify the rationality of aerodynamic and structure model, and the results are shown in Figure 9. The deformation shows that the strut significantly reduces the inner-part displacement of the wing structure.

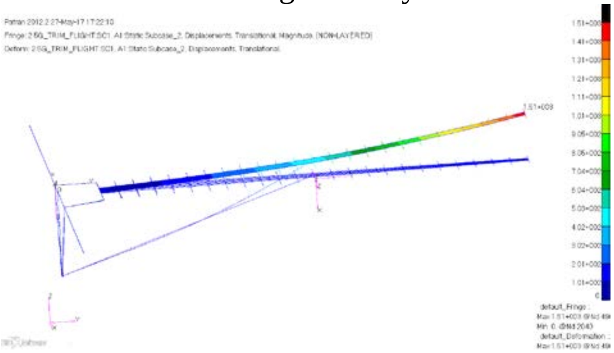

(a) Structure deformation in 2.5g load condition

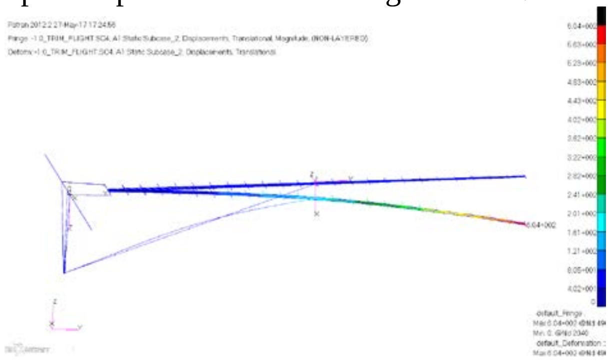

(b) Structure deformation in -1.0g load condition

Figure 9: Structure deformation of aeroelastic analysis

4.2 Optimization results

For all the four positions that the strut-wing intersecting position is set to be, the individuals with highest fitness of given design constraints are re-analyzed and the rationality is confirmed. The structure weight, wing tip displacement, wing tip rotation, aileron efficiency and drag of individuals with highest fitness in each condition are shown as following. The other constraints like flutter speed, Tsai-Wu failure criteria, strain constraint and buckling constraint are met respectively.

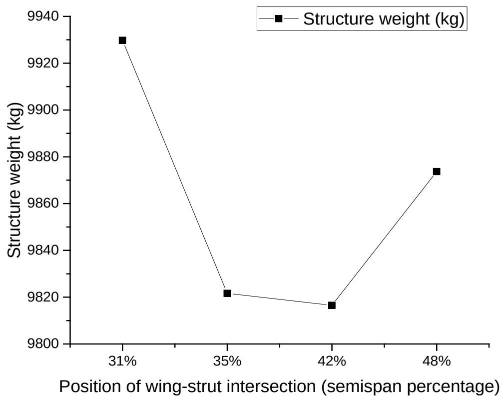

(a) Structure weight in four conditions

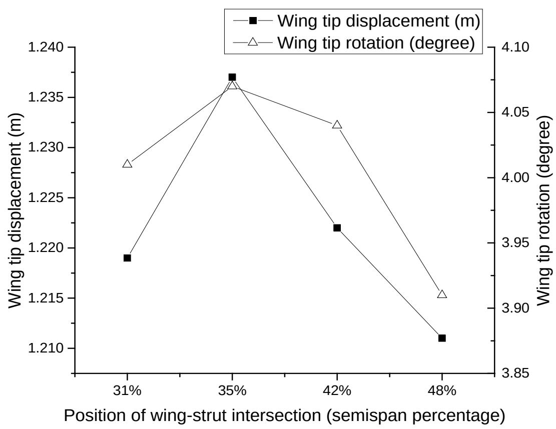

(b) Deformation in four conditions

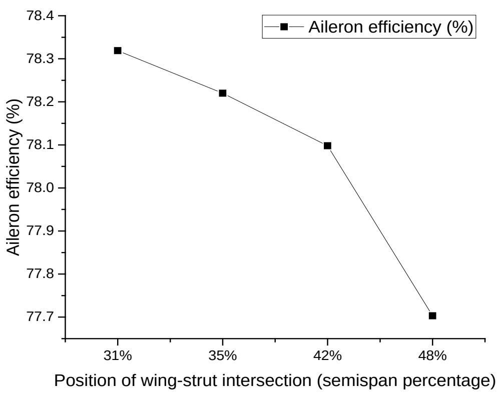

(c) Aileron efficiency in four conditions

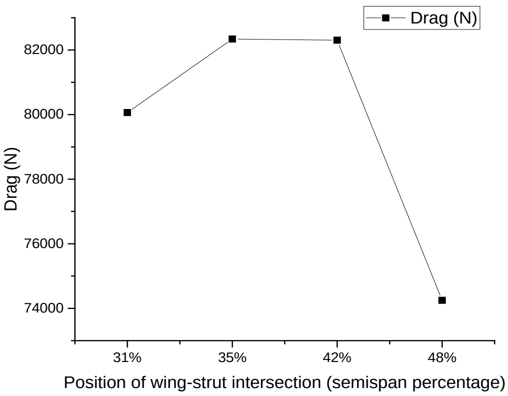

(d) Drag in four conditions

Figure 10: Design responses in four conditions

With the position changes along the spanwise direction, structure deformation including displacement and rotation changes, which is clearly shown in Figure (b), therefore significantly effects the aileron efficiency and drag, which is shown in Figure(c) and Figure (d) respectively. The design of SBW aircraft is not a single index like drag or weight, but the integration of all the indices above, and different weights of each index is applied with the change of task profile and requirement. A compromise of these indices should be made in an actual design process referring to the detailed analysis in conceptual stage.

5 CONCLUTIONS

An MDO method on composite wing structure of SBW commercial aircraft is proposed. The aeroelastic deformation and other indices of SBW aircraft with different design parameters are analyzed. The drag of each individual is analyzed based on the aerodynamic model of cruise configuration. In this genetic algorithm based method, the effects of configuration parameters, composite laminate thickness and section size of main beams are taken into comprehensive consideration. The optimization is divided into four parallel programs with the different position where strut and wing intersected. A contradistinction of weight, drag, wing tip displacement as well as rotation and aileron efficiency of four individuals is presented. Each of the four individuals is the one with the highest fitness of different wing-strut intersecting position. The results demonstrate that the form of aeroelastic deformation of the composite structure effects the aerodynamic performance and other indices, and is significantly affected by the position of wing-strut intersection. In order to get a higher accuracy and avoid repeated iterations, the aeroelasticity and the feature of composite structure should be taken into consideration in conceptual stage. This MDO method can search for optimized values of both configuration and structure property design within acceptable calculate consumption, thus could provide meaningful guiding of configuration and structure design in conceptual stage.

6 ACKNOWLEDGEMENT

This work was supported by the National Key Research and Development Program (2016YFB0200703).

7 REFERENCES

[1] Kulfan R M, Vachal J D. Wing Planform Geometry Effects on Large Subsonic Military Transport Airplanes[R]. BOEING COMMERCIAL AIRPLANE CO SEATTLE WASH, 1978.

[2] Grasmeyer III J M. Multidisciplinary design optimization of a strut-braced wing aircraft[D]. Virginia Tech, 1998.

[3] Gundlac J, Tetrault P A, Gern F, et al. Multidisciplinary design optimization of a strut-braced wing transonic transport[C]//38th aerospace sciences meeting and exhibit. 2000: 420.

[4] Gern F H, Ko A, Sulaeman E, et al. Multidisciplinary design optimization of a transonic commercial transport with strut-braced wing[J]. Journal of aircraft, 2001, 38(6): 1006-1014.

[5] Gern F H, Naghshineh-Pour A H, Sulaeman E, et al. Structural wing sizing for multidisciplinary design optimization of a strut-braced wing[J]. Journal of aircraft, 2001, 38(1): 154-163.

[6] Gundlach J F, Philippe-André, Té, et al. Conceptual design studies of a strut-braced wing transonic transport[J]. Journal of aircraft, 2000, 37(6): 976-983.

[7] Turriziani R V, Lovell W A, Martin G L, et al. Preliminary design characteristics of a subsonic business jet concept employing an aspect ratio 25 strut braced wing[J]. 1980.

[8] Smith P M, DeYoung J, Lovell W A, et al. A study of high-altitude manned research aircraft employing strut-braced wings of high-aspect-ratio[J]. 1981.

[9] Wan Z, Yang C, Zou C. Design studies of aeroelastic tailoring of forward-swept composite aircraft using hybrid genetic algorithm [C] //44th AIAA/ASME/ASCE /AHS/ASC Structures, Structural Dynamics, and Materials Conference. 2003: 1491.

[10] Liang L, Wan Z Q, Yang C. Aeroelastic optimization on composite skins of large aircraft wings[J]. Science China Technological Sciences, 2012, 55(4): 1078-1085.

[11] Stephen W T. Theory of Composites Design[J]. Dayton: Think Composites, 1992: 8-13.

[12] Narayanaswami R, Adelman H M. Evaluation of the tensor polynomial and Hoffman strength theories for composite materials[J]. Journal of Composite Materials, 1977, 11(4): 366-377.

[13] Zhou, M. and Sun, S. D., Genetic Algorithms: Theory and Applications, National Defence Industry Press, Beijing, 1999 (in Chinese).

[14] TIDD D, STRASH D, Epstein B, et al. Application of an efficient 3-D multigrid Euler method (MGAERO) to complete aircraft configurations[C]//9th Applied Aerodynamics Conference. 1991: 3236.

[15] Levy D, Wariner D, Nelson E. Validation of computational Euler solutions for a high speed business jet[C]//12th Applied Aerodynamics Conference. 1994: 1843.

[16] Van Dam C P, Nikfetrat K, Wong K, et al. Drag prediction at subsonic and transonic speeds using Euler methods[J]. Journal of aircraft, 1995, 32(4): 839-845.

[17] Wan Z Q, Wang X Z, Yang C. Integrated aerodynamics/structure/stability optimization of large aircraft in conceptual design[J]. Proceedings of the Institution of Mechanical Engineers, Part G: Journal of Aerospace Engineering, 2017: 0954410016687143.

[18] McCormick C W. The NASTRAN User's Manual (Level 15) [J]. 1972.

[19] Zhiqiang W, Xiaozhe W, Chao Y. A Highly Efficient Aeroelastic Optimization Method Based on a Surrogate Model[J]. International Journal of Aeronautical and Space Sciences, 2016, 17(4): 491-500.

COPYRIGHT STATEMENT